ground water

Coupled Aquifer–Borehole Simulation

by Tom Clemo[1,2]

Abstract

A model coupling fluid hydraulics in a borehole with fluid flow in an aquifer is developed in this paper. Conservation of momentum is used to create a one-dimensional steady-state model of vertical flow in an open borehole combined with radially symmetric flow in an aquifer and with inflow to the well through the wellbore screen. Both laminar and turbulent wellbore conditions are treated. The influence of inflow through the wellbore screen on vertical flow in the wellbore is included, using a relation developed by Siwoń (1987). The influence of inflow reduces the predicted vertical variation in head up to 15% compared to a calculation of head losses due to fluid acceleration and the conventional Colebrook-White formulation of friction losses in a circular pipe. The wellbore flow model is embedded into the MODFLOW-2000 ground water flow code. The nonlinear conservation of momentum equations are iteratively linearized to calculate the conductance terms for vertical flow in the wellbore. The resulting simulations agree favorably with previously published results when the model is adjusted to meet the assumptions of the previous coupled models.

Introduction

This paper describes the mathematical basis of a modified version of MODFLOW-2000 (Harbaugh et al. 2000) that performs a coupled simulation of steady-state flow in an aquifer and vertical flow within a borehole. For simplicity, the aquifer geometry is assumed to be radially symmetric. Flow within the borehole is solved using an iterated one-dimensional finite-difference solution of the nonlinear conservation of momentum equations. The model includes flow energy losses associated with the conversion of radial flow entering the borehole to vertical flow in the borehole, as well as contraction and drag losses in the inflow through a wellbore screen.

Garg and Lal (1971) developed a mathematical description of flow through the aquifer, screen slots, and borehole that has the same fundamental basis as the model presented here. They experimentally verified the validity of the model using a laboratory-scale simulated screened borehole and aquifer. They list five limiting assumptions to their development:

1. Flow is assumed to be laminar within both the wellbore and the aquifer.
2. Flow is radially inward within the aquifer.
3. The velocity within the wellbore is uniform across the pipe cross section.
4. The effect of particles around the well screen that may result in choking can be neglected.
5. All energy of flow entering the screen is lost when the direction is changed from radial flow to the borehole to axial flow within the borehole.

Following the development of Garg and Lal, VonHofe and Helweg (1998a; 1998b) used a finite-difference model of the wellbore flow system to determine an optimal location for a pump inlet within a supply well. They demonstrated that the conventional pumping location near the top of the well is more costly than a location closer to the center of the screened interval. They also verified that the model had practical validity using experimental data from an operating municipal supply well.

Cooley and Cunningham (1979) investigated the influence of flow through the screen and within the

[1]Center for the Investigation of the Shallow Subsurface, Boise State University, 1910 University Dr., Boise, ID 83725-1536
[2]Currently at Intera, Inc., 1933 Jadwin Ave, Suite 130, Richland, WA 99354; 509-946-9898; fax: 509-946-7878; tclemo@intera.com
Received May 2008, accepted May 2009.
Copyright © 2009 The Author(s)
Journal compilation © 2009 National Ground Water Association.
doi: 10.1111/j.1745-6584.2009.00597.x

borehole on the interpretation of transient drawdown from a well. They assumed Darcy flow in the formation and turbulent conditions in the wellbore, with a constant coefficient of drag along the borehole sides. They investigated the applicability of the standard assumption of radial flow to a borehole in conventional modeling approaches. A sensitivity study was performed for a variety of homogeneous hydraulic conductivity values, wellbore properties, and pumping rates. Layered systems with gravel packs about the well were also examined. They found that significant vertical flow components can occur near a pumping well in uniform aquifers with a hydraulic conductivity greater than 0.00025 m/s when the pumping rate exceeds 0.02 m^3/s in a 0.15-m-diameter well. For this well diameter, they concluded that standard aquifer testing assumptions may lead to significant errors in estimating hydraulic conductivity, if the hydraulic conductivity is greater than 0.0005 m/s.

Kaleris (1989) investigated the influences of in-well hydraulics on the inflow to wells with long screened intervals. Whereas Cooley and Cunningham's study was dynamic, Kaleris investigated steady-state flow and provided a more detailed treatment of vertical head losses than Cooley and Cunningham. In the Kaleris development, both laminar and turbulent vertical wellbore flows were considered. The drag coefficients for flow in the wellbore and flow through the screen were treated as functions of flow rate. He used the conventional Colebrook-White (Rouse 1961) formulation of the friction factor for drag losses in a rough cylindrical pipe. Alternately, the Prandtl-Karman equation (Rouse 1961) is used when outflow from the pipe occurs.

One of the innovations introduced by Kaleris was to investigate the influence of vertically variable inflow, introduced by wellbore head losses, on the interpretation of contaminant concentration observed in samples acquired from long-screen monitoring wells. If there is a vertical gradient in the concentration of formation fluids, then the concentration of the fluid pumped from the wellbore is a function of the vertical distribution of inflow rate. His results are presented as plots of inflow rate as a function of distance from the bottom of the screened interval for pumping from either the top or bottom of the screen (Figure 3 of Kaleris [1989]). The ratio of largest to smallest inflow rate is also plotted as a function of flow losses in the well, momentum changes in the well, head losses in the aquifer, and the length of the screened interval (Figures 5 and 6 of Kaleris [1989]). For different assumptions of the vertical distribution of solute concentration in the formation, the concentration measurements show a significant sensitivity to flow conditions in the well. Kaleris et al. (1995) used the model in combination with a nondispersive transport model to investigate the efficacy of several solute sampling systems for both estimation of hydraulic conductivity and interpretation of concentration data.

The flow losses in perforated pipes such as a wellbore screen have a different functional relationship to flow than the formulation for flow in a solid pipe. Siwoń (1987) developed empirical relations for pressure losses of flow in a perforated pipe both with and without flow entering the pipe through the perforations. He developed the relations from an extensive series of experiments on flow into polyvinyl chloride (PVC) drain pipes. He concluded that holes in the pipe wall increase the drag in both laminar and turbulent flow regimes. He also concluded that not all of the energy from lateral inflow is lost. From direct simulation of the Navier-Stokes equations, Friedrich et al. (2001) reached a similar conclusion about the influence of pipe porosity on drag in low Reynolds number turbulent flows. Both studies indicated that the additional drag could be represented with an additional constant term in the friction factor representation.

Lateral inflow into pipes has become an important issue in the oil industry with the advent of horizontal drilling technology. Head losses within the pipes in horizontal wells are relatively more important than with vertical wells (Penmatcha et al. 1997). A number of research groups have conducted experiments to investigate the influence of inflow on pressure losses. Clemo (2006) compared Siwoń's (1987) relations to a variety of experiments on flow losses in perforated pipes and porous tubes both with and without inflow. The relations developed by Siwoń appear accurate for both water and air.

Rehfeldt et al. (1989) investigated the influence of wellbore energy losses and well-screen energy losses on the estimation of vertical distributions of hydraulic conductivity from borehole flowmeters. Their report, drawing on the work of Cooley and Cunningham (1979) and Hufschmied (1983), contains a detailed development of the theory of flow within the borehole through the screen, and the formation. They did not include the influence of wellbore head variations on inflow to the well and highlighted the assumption of radial flow as a limitation of their development. Owing to this limitation, they concluded that the loss calculations are not sufficiently accurate for routine use. The analysis considers the potential effects of a disturbed zone and gravel pack around the well. In addition to the study of wellbore losses, they also presented practical guidelines for the construction of wells for use with flowmeters and for interpretation of hydraulic conductivity from flowmeter measurements.

The model presented here is a further refinement of the model developed by Garg and Lal (1971). Each of the five assumptions listed by Garg and Lal have been relaxed in MODFLOW model, although assumption 4 is relaxed only by use of a user supplied parameter. It improves on the refinements made by Cooley and Cunningham (1979) and Kaleris (1989). The wellbore model is improved from Kaleris's model with the replacement of the Colebrook-White formulation for the friction factor with Siwoń's relations. The model also incorporates the screen loss analysis of Rehfeldt et al., which is extended to consider possible clogging of the screen. The model, implemented within MODFLOW-2000, includes the interaction of wellbore flow with flow within the formation overcoming the radial flow limitation cited by Rehfeldt et al. (1989).

Halford introduced a turbulent flow module for MODFLOW to investigate interaction between flowmeter, well, and aquifer (Halford 2000). Effective hydraulic conductivities and resulting conductances were calculated for well, screen, and annular space. Turbulent losses were simulated with an effective hydraulic conductivity term that was a function of Reynolds number and implemented in a look-up table. Halford's implementation is a simpler approximation than the approach described in this paper but may be more efficient. Mode 2 of the conduit flow process in MODFLOW-2005 also simulates turbulence using Halford's hydraulic conductivity approach (Shoemaker et al. 2008).

Formulation of Borehole Flow Equations

The model is separated into two regions. Within the formation, flow is described by the ground water flow equations in radially symmetric cylindrical coordinates. Reilly and Harbaugh (1993a) described the formulation of the finite-difference equations for cylindrical geometry that were incorporated into a preprocessor for MODFLOW-96 called RADMOD (Reilly and Harbaugh 1993b). Preprocessing to convert the finite-difference equations to cylindrical geometry is also used by Langevin (2008) for both flow and transport. Specifics of the implementation within MODFLOW are documented in a report on the cylindrical geometry version of the MODFLOW-2000 code that does not include the borehole flow model (Clemo 2002). The innermost column of the MODFLOW model represents the borehole. Within the borehole, a one-dimensional finite-difference formulation of momentum conservation equations is used to simulate vertical flow. At the boundary between the open borehole and the formation, a one-dimensional formulation of momentum conservation equations is used to simulate radial flow through a screen and into the borehole.

An understanding of the important physical processes that influence flow in the open borehole and through the screen can be gained through the investigation of momentum conservation within a borehole section as shown in Figure 1. In Figure 1, z_1 and z_2 are elevations and p_1 and p_2 represent the fluid pressure at the bottom and top of the control volume; r_w is the radius of the wellbore; and $p(z)$ is the vertical pressure distribution. $v_z(r)$ represents the radially dependent vertical velocity distribution; it is drawn in the figure with a parabolic distribution of laminar flow. V is the bulk (average) velocity of the wellbore as defined in Equation 4. v_r is the radial velocity just inside the screen. Although written with a radial direction subscript, the velocity direction may vary from horizontal by an angle γ. τ_w represents drag forces operating on the fluid at the wall of the screen.

Momentum conservation is simply a restatement of the relation $F = ma$. The momentum equation is expressed as (Parker et al. 1969):

$$\frac{D}{Dt}\int_{\mathrm{Vol}} \rho v\, d(\mathrm{Vol}) = \sum forces \qquad (1)$$

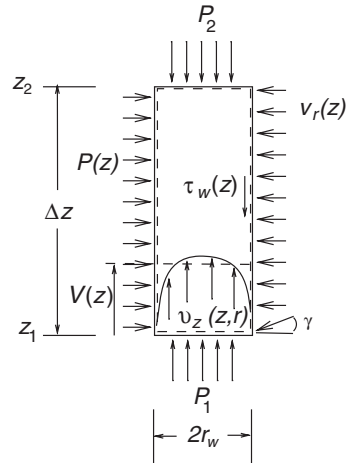

Figure 1. Momentum balance control volume for a wellbore.

where ρ is the density of fluid, v is the velocity, and the forces are both external and body forces. $\frac{D}{Dt}$ is the substantial derivative. Equation 2 separates the substantial derivative into two components: the change in internal momentum within the volume and the flux of momentum across the boundaries of the volume.

$$\frac{D}{Dt}\int_{\mathrm{Vol}} \rho V v d(\mathrm{Vol}) = \frac{\partial}{\partial t}\int_{\mathrm{Vol}} \rho v d(\mathrm{Vol}) + \int_{\Omega} \rho v (v \cdot n) \mathrm{d}\Omega \qquad (2)$$

where Ω represents the volume's surface and $v \cdot n$ is the component of velocity normal to the surface.

Change in Momentum

The conservation of momentum is a vector equation, which must be satisfied in each direction. Axial symmetry ensures agreement in the radial direction. With the assumption of steady incompressible flow, the derivative with respect to time is zero and Equation 2 can be rewritten for the axial direction as

$$\frac{D}{Dt}\int_{\mathrm{Vol}} \rho v d(\mathrm{Vol}) = \rho 2\pi \int_{o}^{r_w} v_z^2 r \mathrm{d}r \Big|_{z_2} - \rho 2\pi \int_{o}^{r_w} v_z^2 r \mathrm{d}r \Big|_{z_1} + \rho 2\pi r_w \int_{z_1}^{z_2} v_z \cdot v_r \mathrm{d}z \qquad (3)$$

The first term on the right represents the momentum flux across the lower boundary of the volume. The second term is the momentum flux exiting through the top boundary. The last term is the momentum introduced by fluid inflow through the screen. Recognizing that the flow in the pipe increases due to inflow, $\frac{\partial v_z}{\partial z} = \frac{2\pi r_w}{\pi r_w^2} v_r$, the vector product $v_z \cdot v_r$ can be rewritten as $\frac{1}{2\pi r_w^2} v_r^2 \sin(2\gamma)$. If the inflow through the slot is perpendicular to the direction of flow, then γ is 0° and the last term on the right-hand side of Equation 3 drops out.

The average or bulk velocity is defined as

$$V = Q/\pi r_w^2 \qquad (4)$$

To proceed, a spatial distribution of flow velocities is needed. In pipes with solid walls, the distribution of velocity can be calculated for laminar flow and has been found experimentally under turbulent flow conditions. Under laminar flow conditions, the velocities follow a parabolic distribution (Parker et al. 1969):

$$v_z = 2V\left(1 - \frac{r}{r_\mathrm{w}}\right) \tag{5}$$

resulting in

$$\rho 2\pi \int_o^{r_\mathrm{w}} v_z^2 r \mathrm{d}r = \frac{4}{3}\rho\pi r_\mathrm{w}^2 V^2 \tag{6}$$

From the experimental data of Nikuradse (Nikuradse 1932; Parker et al. 1969), the velocity profile of turbulent flow in a pipe has the form

$$\frac{v_z}{v_{cl}} = \left(\frac{r}{r_\mathrm{w}}\right)^{\frac{1}{n}} \tag{7}$$

with v_{cl} being the velocity at the center of the pipe and with n increasing from 6 to 7 as the Reynolds number increases from 4000 to 100,000. Integrating across the wellbore cross-sectional results in

$$\rho 2\pi \int_o^{r_\mathrm{w}} v_z^2 r \mathrm{d}r = \beta\rho\pi r_\mathrm{w}^2 V^2 \tag{8}$$

where β is referred to as the momentum factor. Streeter (1950) developed an equation for the momentum factor for turbulent flow in a pipe as a function of the friction factor (see Equations 13 and 14):

$$\beta = 1. + 0.98\, f \tag{9}$$

Equations 5 through 9 do not consider the effect of openings or inflow through the slots on the velocity profile.

We now focus on the influence of inflow on momentum of the flow in the pipe. Olson and Eckert (1966) investigated the velocity profile for air inflow into a porous tube. They considered pressure changes in their experiment to be insignificant and analyzed the data using incompressible flow equations. When inflow entered a tube with a fully developed velocity profile, a new profile evolved within a distance of six to eight pipe diameters with a momentum factor described by

$$\beta = 1.034 + 4.27\frac{v_r}{V} \tag{10}$$

over a range of $\frac{v_r}{V}$ from 0.002 to 0.017. Beyond this range, β reached a plateau of approximately 1.11. When inflow entered a tube that was blocked at the upstream end, the velocity profile had a momentum factor of 1.08 almost immediately and then evolved to 1.11. With no inflow through the walls, a β of 1.024 was determined from the velocity measurements. This is consistent with Equation 9, which predicts a β of 1.024 for the friction factor of 0.025 determined by Olson and Eckert for the tube by measuring the pressure drop.

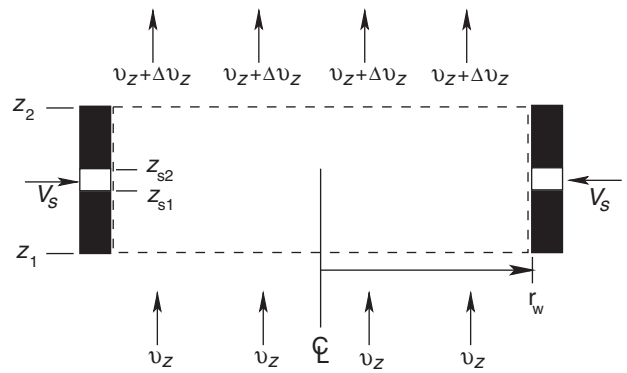

Figure 2. Small control volume for one section of a screened wellbore.

Figure 2 depicts a small control volume that isolates an individual slot opening in the wellbore screen. V_s is the average fluid velocity in the slot. The flow at the top of the section differs from the bottom by the inflow through the slot. The change in bulk flow is $V_2 - V_1 = \frac{2\alpha_r(z_{s1}-z_{s2})V_\mathrm{s}}{r_\mathrm{w}}$ where α_r is the fraction of the radius open to flow. Subscripts 1 and 2 refer to the bottom and top of the volume, respectively, which are located half way between slots. The z_{s1} and z_{s2} are the elevations of the bottom and top of the slot. The velocity in the pipe at the wall, v_r, in Equation 10 is related to average inward velocity through the slot by the porosity of the screen, $\phi = \frac{2\alpha_r(z_{s2}-z_{s1})}{(z_2-z_1)r_\mathrm{w}}$. The inflow term in Equation 3 can also be written in terms of these variables as

$$\rho\frac{2}{r_\mathrm{w}}\int V_\mathrm{s}^2 \sin(2\gamma)\,\mathrm{d}z = \rho\frac{4\alpha_r}{r_\mathrm{w}}(z_{s1} - z_{s2})\, V_\mathrm{s}^2 \sin(2\overline{\gamma}) \tag{11}$$

$\overline{\gamma}$ is an effective average angle over the cross section of the slot.

Sum of Forces

We now turn to the force aspect of the conservation of momentum. The forces acting on the fluid in Equation 1 are gravity, pressure along the top and sides, and shear along the sides. These forces are respectively represented by the three terms on the right-hand side of Equation 12.

$$\begin{aligned}\rho 2\pi \int_o^{r_\mathrm{w}} v_z^2 r \mathrm{d}r\Big|_{z_2} - \rho 2\pi \int_o^{r_\mathrm{w}} v_z^2 r \mathrm{d}r\Big|_{z_1} \\ +\rho 4\pi r_\mathrm{w}\alpha_r (z_{s1} - z_{s2})\, V_\mathrm{s}^2 \sin(2\overline{\gamma}) = -\rho g\pi r_\mathrm{w}^2 \Delta z \\ +\pi r_\mathrm{w}^2 (p_1 - p_2) - 2\pi r_\mathrm{w}\int_{z_1}^{z_2} \tau_\mathrm{w}\mathrm{d}z\end{aligned} \tag{12}$$

where $\Delta z = z_2 - z_1$ is the length of the section, p_1 and p_2 are fluid pressures at the bottom and top of the section, and τ_w is the average shear stress along the surface of the inner screen. The average shear stress may be written in terms of the Fanning friction factor, f (Cooley and Cunningham 1979; Kaleris 1989).

$$\tau_\mathrm{w} = \frac{\rho f V^2}{8} \tag{13}$$

The friction factor is commonly described for a circular pipe by (Parker et al. 1969; Kaleris 1989)

$$\begin{aligned} f &= \frac{64}{Re} \quad Re < Re_{\text{lam}} \quad \text{Laminar flow} \\ f^{-\frac{1}{2}} &= -2\log\left[\frac{\epsilon_p}{3.71} + \frac{2.51}{Re} f^{-\frac{1}{2}}\right] \\ & \quad Re > Re_{\text{turb}} \quad \text{Turbulent flow} \end{aligned} \tag{14}$$

where ϵ_p is the relative roughness of the pipe. The Reynolds number, Re, is defined as $Re = \frac{V d_h}{\nu}$, where ν is the kinematic viscosity and d_h is the diameter of the pipe. The transition region between laminar to turbulent flow occurs between $Re_{\text{lam}} > 2000$ and $Re_{\text{turb}} < 4000$. The relation for laminar flow follows from a parabolic velocity distribution and has been verified experimentally. The relation for turbulent flow is known as the Colebrook-White formula (Rouse 1961). Experimental and theoretical evidence indicates that the friction factor is different for perforated pipes (Siwoń 1987; Su 1996; Yuan 1997; Friedrich et al. 2001) from the friction factor in solid wall pipes.

Siwoń (1987) developed a relation for the friction factor for drilled PVC pipe as

$$f = f_0 + f_t \tag{15}$$

where $f_0 = 0.0106\,\phi^{0.413}$ and f_t is given by Equation 14 with $\epsilon = \epsilon_p + 0.282\phi^{2.4}$ for $Re > 3400$. ϕ is the perforation density (fraction of the screen open to radial flow). Siwoń experimented with different configurations of opening and found that f_0 and f_t were insensitive to the configurations. This insensitivity to perforation geometry may not hold for all geometries (Clemo 2006). The treatment of wall openings with an effective roughness factor is in agreement with the numerical study of Friedrich et al. (2001). They used numerical solution of the Navier-Stokes equations to investigate the effect of wall openings.

Figure 4 of Siwoń (1987) shows that experimentally derived f_t follows an almost linear variation with log(Re) between the end of laminar flow ($Re = 2260$) and the beginning of turbulent flow, at $Re = 3400$. This smooth relation may represent the averaging over finite lengths of measurement. This is a region of transient turbulence even though the flow is considered steady state (Eckhardt et al. 2007; Rouse 1961). No fit is presented by Siwoń (1987) for this range. The relation used here is an interpolation across this range that varies linearly with respect to $\log(Re)$.

$$\begin{aligned} f &= f_0 + 0.028 + \frac{\log(Re) - 3.354}{0.177} \\ & \quad \times (f_t(\epsilon, 3400) - 0.028) \end{aligned} \tag{16}$$

Conservation of Momentum

The definitions provided so far can now be used to formulate the conservation of momentum equations used in the model. Combining Equations 12, 5 or 7, and 13 results in

$$\begin{aligned} &\beta_2 \rho \pi r_{\text{w}}^2 V_2^2 - \beta_1 \rho \pi r_{\text{w}}^2 V_1^2 + \rho 4\pi r_{\text{w}} \alpha_r (z_{s1} - z_{s2}) \\ &\quad \times V_{\text{s}}^2 \sin(2\overline{\gamma}) = \rho g \pi r_{\text{w}}^2 (h_2 - h_1) \\ &\quad + \frac{\rho \pi r_{\text{w}}}{4} \int_{z_1}^{z_2} f\, V^2 \mathrm{d}z \end{aligned} \tag{17}$$

where hydraulic head, $h = z + \frac{p}{\rho g}$, is used to replace the elevation and fluid pressure terms, and β represents the appropriate factor to account for velocity distribution. Reorganizing in terms of the head difference gives

$$\begin{aligned} h_2 - h_1 &= \frac{\beta_2 V_2^2}{g} - \frac{\beta_1 V_1^2}{g} + \frac{4\pi r_{\text{w}} \alpha_r (z_{s1} - z_{s2}) V_{\text{s}}^2}{g} \\ & \quad \times \sin(2\overline{\gamma}) - \frac{1}{4 g r_{\text{w}}} \int_{z_1}^{z_2} f\, V^2 \mathrm{d}z \end{aligned} \tag{18}$$

Experimental studies have been conducted to investigate the influence of inflow on the head drop along a segment of pipe (Siwoń 1987; Su 1996; Su and Gudmundsson 1998; Yuan 1997; Yuan et al. 1999; Ouyang 1998). All of these investigations indicate that the head drop is less than would be the case if β and f were unaffected by inflow and $\hat{\gamma}$ was zero. None of these investigations was of sufficient detail to distinguish between the various terms contributing to the total head drop. Su and Gundmundsson (1998), Ouyang (1998), and Ouyang et al. (1998) assumed that the friction factor is reduced by inflow. Experiments with air flow in porous pipes (Olson and Eckert 1966) and numerical calculation of shear stresses at the wall of a pipe with inflow (Arif 1999) support this assumption. Siwoń attributed the lower head losses to the discontinuity of inflow and the angle of inflow. The experimental study of orifice coefficients from a perpendicular flow field (Andrews and Sabersky 1990; Strakey and Talley 1999) gives some support for Siwoń's attribution, but the support for a reduced friction factor is much stronger. Both influences are likely. At present the causes are not separable. To model flow in the wellbore, only a composite effect is needed—not the underlying causes.

Siwoń conducted an investigation of the head losses in drilled PVC pipes used as drains. He developed a series of empirical relations for the variation of head considering inflow through the holes. The inflow is assumed to be uniform over the section at the scale of a model element. The various experiments listed previously strongly support the validity of this important simplification (Clemo 2006). His relation effectively combines the first three terms in Equation 18 to form an equation for the head drop across the volume as

$$h_2 - h_1 = \eta(V_1, V_2) \frac{V_2^2 - V_1^2}{2g} - \frac{1}{4 g r_{\text{w}}} \int_{z_1}^{z_2} f\, V^2 \mathrm{d}z \tag{19}$$

where η is defined as

$$\eta(V_1, V_2) = \frac{1}{1 - \left(\frac{v_1}{v_2}\right)^2} \left[c(\phi, \frac{V_2}{v_r}) - \left(\frac{V_1}{V_2}\right)^2 c(\phi, \frac{V_1}{v_r}) \right] \tag{20}$$

in which

$$c\left(\phi, \frac{V}{v_r}\right) = 1.05 + \left\{\left[\left(\frac{10}{(10^3\phi)^{4.2}} + \frac{4}{10^7}\right)\left(\frac{V}{v_r}\right)^2\right] + 1.235\right\}^{-1} \quad (21)$$

for small inflows, $\frac{V}{v_r} \gg \left(\frac{10}{(10^3\phi)^{4.3}} + \frac{4}{10^7}\right)$, c approaches 1.05, and for large inflows, $\frac{V}{v_r} \ll \left(\frac{10}{(10^3\phi)^{4.3}} + \frac{4}{10^7}\right)$ and c approaches 1.86. Clemo (2006) demonstrates that Siwoń's formulation is consistent for $\frac{V}{v_r}$ ratios greater than 40 for a wide range of experimental results.

Head Loss across the Screen

The development presented here for head loss across the screen follows that of Rehfeldt et al. (1989). Two processes cause a decrease in head from the formation to the open wellbore. Shear forces from flow through the slot cause part of the head loss. Kinetic energy and shear losses from expansion and contraction of flow both entering and exiting the slot cause the other part of the loss. The shear forces in the slot can be represented by a modified form of the Fanning friction factor for circular pipes as (Rehfeldt et al. 1992):

$$f_s = C_E \psi f \quad (22)$$

where C_E is an experimentally determined correction factor and ψ is a form factor dependent on the slot geometry. The C_E factor is based on the work of Klotz (1977). Rehfeldt et al. report for laminar flow that

$$C_E = 10^{\left[\frac{A \log_{10} \frac{r_{sH}}{OD} + B}{\left[\frac{100}{ID+OD}\right]^2}\right]} \quad (23)$$

where ID is the inner diameter and OD is the outer diameter of the screen and r_{sH} is the hydraulic radius of the slot defined as

$$r_{sH} = \frac{2A}{Cir} = \frac{(z_{s2} - z_{s1})\, W_s}{(z_{s2} - z_{s1}) + W_s} \quad (24)$$

where A is the cross-sectional area of the slot and Cir is the circumference of the slot opening as determined for the average of the slot. See Figure 3 for depictions of the variables.

From a literature investigation, Hufschmied (1983) concluded that the critical Reynolds number for a circular pipe is also appropriate for flow through the slot. Based on this number, Rehfeldt et al. determined that, for their investigation of well testing hydraulics at the MADE site, flow in well-screen slots was always laminar. Kaleris et al. (1995) also assumed laminar flow in the well-screen slots. In the modified MODFLOW code, the friction factor for the slot is determined from Equation 14 using V_s and r_{sH}

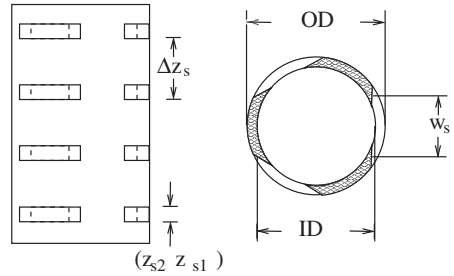

Figure 3. Schematic diagram of well-screen slot geometry.

of the slot in place of V and r_w of the wellbore. The model is, therefore, also appropriate for the turbulent screen conditions to be expected in supply wells. The factor C_E is applied in both circumstances. The coefficient C_E is an input parameter to the model allowing relations other than Equation 23 to be used. The Reynolds number for the slot was always below the critical Reynolds number for the simulations presented in the following text.

An equation for the form factor, ψ, was developed by Richter (1971).

$$\psi = \frac{3r_{sH}^2}{2(z_{s2} - z_{s1})^2}\left[1 - \frac{192(z_{s2} - z_{s1})}{\pi^5 W_s} \times \left[\tanh\frac{\pi W_s}{2(z_{s2} - z_{s1})} + \frac{1}{3^5}\tanh\frac{3\pi W_s}{2(z_{s2} - z_{s1})} + \ldots\right]\right]^{-1} \quad (25)$$

For square openings, that is, $W_s = (z_{s2} - z_{s1})$, then $\psi = 0.889$. For narrow slots with $W_s \gg (z_{s2} - z_{s1})$, then $\psi = 1.5$.

Expansion and contraction losses for thin orifices are well known (Crane Co. 1988). These losses occur because the fluid must accelerate to squeeze through the slot (a process opposed by shear forces related to the viscosity of the fluid), and the kinetic energy in the accelerated flow is lost when the flow enters the volume downstream of the orifice. The flow through an orifice is given by (Crane Co. 1988)

$$q = -\frac{C_d A}{\sqrt{1 - \frac{A_1}{A_2}}}\sqrt{2g\Delta h} \quad (26)$$

where q is the rate of flow, A is the cross-sectional area of the orifice, $\frac{A_1}{A_2}$ is the ratio of the narrowest area of the orifice to the upstream area of flow, C_d is an empirically defined discharge coefficient, and $\frac{1}{\sqrt{1-\left(\frac{A_1}{A_2}\right)^2}}$ is the velocity coefficient, C_v of Rehfeldt et al. (1989). C_d has a value of approximately 0.72 (Rehfeldt et al. 1989; Rouse 1961) for slotted well screens. The definition of A_2 is ambiguous for radially contracting flow in a porous media. It is removed using C_v to obtain

$$\Delta h = -C_d^{-2} C_v^{-2} \frac{\frac{q^2}{A^2}}{2g} \quad (27)$$

The cross-sections A and A_1 in Equation 26 should both be defined at the entry to the slot where the soil grains partially block the entrance of the slot, $A = A_1 \simeq \theta A_s$, of Cooley and Cunningham (1979). The factor Θ represents the fraction of the slot entrance, A_s, open to flow. The product $C_d C_v$ is insensitive to $\frac{A_1}{A_2}$ below 0.2, which is the case for slotted screens. This results in

$$\Delta h = -C_d^{-2} C_v^{-2} \theta^{-2} \frac{V_s^2}{2g} \tag{28}$$

which is in essence the definition developed by Vaadia and Scott (1958) and used by Cooley and Cunningham (1979).

The combined head drop from both shear and orifice losses is

$$\Delta h = -\left(f_s + C_d^{-2} C_v^{-2} \theta^{-2}\right) \frac{V_s^2}{2g} \tag{29}$$

Implementation Verification

The previous calculations of Cooley and Cunningham (1979) and Kaleris et al. (1995) are used to test the implementation. The characteristics of the simulated aquifer are a homogeneous hydraulic conductivity of $5.1 \times 10^{-4} \frac{m}{s}$, a thickness of 30.5 m, and a well radius of 0.0762 m. The results of the calculations are presented in Table 1. The Δh columns refer to the head difference between the top and bottom of the well. The column v_r^{top} is the inflow through the slots at the top of the well and v_r^{bot} refers to inflow at the bottom of the well. The MODFLOW model was revised to provide agreement with the formulation of Cooley and Cunningham (1979). The important changes are as follows: flow is always turbulent with a constant friction factor of 0.05, the β factor is set to 1, slot shear losses are not included, the combined value of $C_d C_v$ is set to 0.61 and, $\theta = 0.1$. The revised model calculations agree closely with the earlier calculations except for slightly higher flow near the top of the aquifer. This disagreement may be a definition problem. To calculate the top and bottom flow rates, layers only 0.01 m thick were used in the revised model. It is not clear whether the other calculations are actually at the top of the model domain or the average for a top layer. Inflow at the top of the model is a strong function of position whereas the flow at the bottom is nearly constant, so the layer thickness is more important at the top. The revised model agreement with previous calculations provides confidence that the use of the CR and CV conductances appropriately merges the in-well momentum equations with the ground water flow equations.

Table 2 indicates changes in the results due to the improvements introduced by Kaleris et al. and this work. Kaleris et al. introduced flow-dependent drag from the walls and through the screen using the Colebrook-White friction factor. These improvements result in approximately 20% smaller head variation in the well and consequently less vertical variation in incoming flow compared

Table 1
Comparison of the Cooley and Cunningham, Kaleris et al., and Modified MODFLOW Models for Cooley and Cunningham's Test Case

Q $\frac{m^3}{s}$	Δh m	v_r^{top} $\frac{m}{s}$	v_r^{bot} $\frac{m}{s}$	Δh m	v_r^{top} $\frac{m}{s}$	v_r^{bot} $\frac{m}{s}$	Δh m	v_r^{top} $\frac{m}{s}$	v_r^{bot} $\frac{m}{s}$
	Cooley and Cunningham			Kaleris et al.			MODFLOW		
$\times 10^{-2}$		$\times 10^{-2}$	$\times 10^{-2}$		$\times 10^{-2}$	$\times 10^{-2}$		$\times 10^{-2}$	$\times 10^{-2}$
2.69	0.565	2.60	1.67	0.585	2.60	1.67	0.557	2.63	1.65
4.39	1.455	5.00	2.57	1.5	4.99	2.55	1.426	5.11	2.55
5.60	2.312	7.05	3.13	2.385	7.04	3.12	2.274	7.25	3.12

Note: The Kaleris et al. model and the MODFLOW models were modified to agree with the assumptions of Cooley and Cunningham. The $\times 10^{-2}$ factors are multipliers that apply to the numbers listed below them.

Table 2
Comparison of Kaleris et al. and Modified MODFLOW Model (Siwoń) to the Cooley and Cunningham Test Case without Adopting the Cooley and Cunningham Assumptions

Q $\frac{m^3}{s}$	Δh m	v_r^{top} $\frac{m}{s}$	v_r^{bot} $\frac{m}{s}$	Δh m	v_r^{top} $\frac{m}{s}$	v_r^{bot} $\frac{m}{s}$
		Kaleris Model			Siwoń Model	
2.69×10^{-2}	0.454	2.46×10^{-2}	1.68×10^{-2}	0.387	2.35×10^{-2}	1.70×10^{-2}
4.39×10^{-2}	1.118	4.68×10^{-2}	2.61×10^{-2}	1.000	4.40×10^{-2}	2.66×10^{-2}
5.60×10^{-2}	1.884	6.57×10^{-2}	3.22×10^{-2}	1.599	6.10×10^{-2}	3.29×10^{-2}

to the Cooley and Cunningham model. Using the more accurate representation of wall shear similar to the development of Kaleris et al. plus Siwoń's formulation, the model described in this paper predicts even less head variation in the well: approximately 30% less than the Cooley and Cunningham model. The results do not contradict the conclusion of Cooley and Cunningham that well losses can significantly influence the inflow distribution to a well in an aquifer with large hydraulic conductivity.

Conclusions

This paper presents a more accurate formulation of flow losses in an open borehole than has been previously described in the ground water literature. The main improvement is the addition of the influence of inflow through the wellbore screen on flow losses that were developed by Siwoń (1987). This formulation predicts smaller wellbore losses than previous models, but the main conclusion of earlier work that borehole losses can be significant in highly permeable aquifers has not changed. With the advent of directional drilling technology, determination of head losses in long sections of collector pipe has become an important issue in the oil industry and presumably in the environmental remediation industry.

Acknowledgments

I am grateful for discussions and collaboration with Vassilios Kaleris on development of the model. This work was supported by U.S. Army Research office grants DAAH04-96-1-0318 and DAAD19-00-1-0454. I am also indebted to Keith Halford and an anonymous reviewer for significantly improving the presentation of the model in this paper.

References

Altshul, A., and P. Kiselev. 1975. *Hydraulics and Aerodynamics*, 2nd ed. USSR: Stroisdat Publishing House.

Andrews, K. and R. Sabersky. 1990. Flow through an orifice from a transverse stream. In *Proceedings of the Winter Annual Meeting*, number 90-WA/FE-3. New York: American Society of Mechanical Engineers.

Arif, H. 1999. Application of computational fluid dynamics (CFD) to the modeling of flow in horizontal wells. Master's thesis, Stanford University, Palo Alto, California.

ASHRAE. 1997. *Fundamentals Handbook*, chapter 32: Duct design. Atlanta, Georgia: American Society of Heating, Refrigerating and Air-Conditioning.

Barrash, W., T. Clemo, J. Fox, and T. Johnson. 2006. Field, laboratory, and modeling investigation of the skin effect at wells with slotted casing, Boise Hydrogeophysical Research Site. *Journal of Hydrology* 326, 181–198.

Chen, N. 1979. An explicit equation for friction factor in pipe. *Industrial and Engineering Chemistry Fundamentals* 18, no. 3: 296–297.

Clemo, T. 2006. Flow in perforated pipes: A comparison of models and experiments. *SPE Production & Operations* 21, no. 2: 302–311.

Clemo, T. 2002. MODFLOW-2000 for cylindrical geometry with internal flow observations and improved water table simulation. Technical Report BSU CGISS 02-01, Center for the Investigation of the Shallow Subsurface. http://cgiss.boisestate.edu/pubs/CGISS_Techreports.html.

Cooley, R., and A. Cunningham. 1979. Consideration of total energy loss in theory of flow to wells. *Journal of Hydrology* 43, 161–184.

Crane Co. 1988. Flow of fluids through valves, fittings, and pipe. Technical Paper 410. Long Beach, California: Crane Company.

Eckhardt, B., T. Schneider, B. Hof, and J. Westerweel. 2007. Turbulence transition in pipe flow. *Annual Review of Fluid Mechanics* 39, 447–468.

Friedrich, R., T. Hüttl, M. Manhart, and C. Wagner. 2001. Direct numerical simulation of incompressible turbulent flows. *Computers and Fluids* 30, 555–579.

Garg, S. and J. Lal. 1971. Rational design of well screens. *Journal of the Irrigation and Drainage Division Proceeding of the American Society of Civil Engineers* 97, 131–147.

Halford, K. 2000. Simulation and interpretation of borehole flowmeter results under laminar and turbulent flow conditions. In *Seventh International Symposium on Logging for Minerals and Geotechnical Applications*, Golden, Colorado, 157–168.

Harbaugh, A., E. Banta, M. Hill, and M. McDonald. 2000. MODFLOW-2000, the U.S. Geological Survey modular ground-water model—User guide to modularization concepts and the ground-water flow process. Open File Report 00-92. Denver, Colorado: USGS.

Hufschmied, P. 1983. Die Ermittlung der Durchlässigkeit von Lockergesteins-Grundwasserleitern, eine vergleichende Untersuchung verschierener Felmethoden. Ph.d., ETH Zurich.

Kaleris, V. 1989. Inflow into monitoring wells with long screens. In *Contaminant Transport in Groundwater*, ed. H. Kobus and W. Kinzelbach, 41–50. Rotterdam: International Association for Hydraulic Research, Balkema.

Kaleris, V., C. Hadjitheodorou, and A. Demetracopoulos. 1995. Numerical simulation of field methods for estimating hydraulic conductivity and concentration profiles. *Journal of Hydrology* 171, 319–353.

Klotz, D. 1977. Berechnete durchlassigkeiten handelgublicher brunnenfilterrohre. Gesellschaft für Strahlen-und Umweltforschung mbH, 133.

Langevin, C. 2008. Modeling axisymmetric flow and transport. Ground Water 46, no. 4: 579–590.

Nikuradse, J. 1932. Gesetzmässigketiten der turbulenten Strömung in glatten Rohren. VDI-Forshungsheft 361, Berlin.

Olson, R., and E. Eckert. 1966. Experimental studies of turbulent flow in a porous circular tube with uniform fluid injection through the tube wall. *Journal of Applied Mechanics* 33, no. 1: 7–17.

Ouyang, L.-B. 1998. Single phase and multiphase fluid flow in horizontal wells. Ph.D. diss., Stanford University, Palo Alto, California.

Ouyang, L.-B., S. Arbabi, and K. Aziz, 1998. A single-phase wellbore-flow model for horizontal, vertical and slanted wells. *SPE Journal* 3, 124–133.

Ouyang, L.-B., and K. Aziz. 1996. Steady-state gas flow in pipes. *Petroleum Science and Engineering* 14, 137–158.

Parker, J., J. Boggs, and E. Blick. 1969. *Introduction to Fluid Mechanics and Heat Transfer*. Reading, Pennsylvania: Addison-Wesley.

Penmatcha, V., S. Arbabi, and K. Aziz. 1997. Effects of pressure drop in horizontal wells and optimum well length. In *1997 SPE Production Operations Symposium, Society of Petroleum Engineers*, number SPE 37494. Oklahoma City, Oklahoma: SPE.

Rehfeldt, K., J. Boggs, and L. Gelhar. 1992. Field study of dispersion in a heterogeneous aquifer. 3. Geostatistical analysis of hydraulic conductivity. *Water Resources Research* 28, no. 12: 3309–3324.

Rehfeldt, K., P. Hufschmied, L. Gelhar, and M. Scheafer. 1989. Measuring hydraulic conductivity with borehole flowmeter. Topical Report no. EN-6511. Palo Alto, California: Electric Power Research Institute, Palo Alto, CA.

Reilly, T., and A. Harbaugh. 1993a. Simulation of cylindrical flow to a well using the U.S. Geological Survey modular finite-difference ground-water flow model. *Ground Water* 31, no. 3: 489–494.

Reilly, T. and A. Harbaugh. 1993b. Source code for the computer program and sample data set for the simulation of cylindrical flow to a well using the U.S. Geological Survey modular finite-difference ground-water flow mode. USGS Open-file Report 92-659. Reston, Virginia: USGS.

Richter, M. 1971. *Rohrhydraulik*. Berlin: Spinger.

Rouse, H. 1961. *Fluid Mechanics for Hydraulic Engineers*. New York: Dover.

Shoemaker, W., E. Kuniansky, S. Birk, S. Bauer, and E. Swain. 2008. Documentation of a conduit flow process (cfp) for modflow-2005. Techniques and Methods 6-A24. Reston, Virginia: USGS.

Siwoń, Z. 1987. Solutions for lateral inflow in perforated conduits. *Journal of Hydraulic Engineering* 113, no. 9: 1117–1132.

Strakey, P., and D. Talley. 1999. The effect of manifold cross-flow on the discharge coefficient of sharp edged orifices. *Atomization and Sprays* 9, 51–68.

Streeter, V. 1950. Steady flow in pipes and conduits. In *Engineering Hydraulics*, ed. H. Rouse. New York: John Wiley & Sons.

Su, Z. 1996. Pressure drop in perforated pipes for horizontal wells. Ph.D. diss., Norwegian University of Science and Technology, Trondheim, Norway.

Su, Z., and J. Gudmundsson. 1998. Perforation inflow reduces frictional pressure loss in horizontal wellbores. *Petroleum Science & Engineering* 19, 223–232.

Vaadia, Y., and V. Scott. 1958. Hydraulic properties of perforated well casings. Journal of the Irrigation and Drainage Division, Proceeding of the American Society of Civil Engineers, 84(IR 1, Paper 1505): 1505.1–1505.26.

VonHofe, F., and O. Helweg. 1998a. Modelling well hydrodynamics. *Journal of Hydraulic Engineering* 124, no. 12: 1198–1202.

VonHofe, F., and O. Helweg. 1998b. The WELLSIM model for analyzing well hydrodynamics. In *Water Resorces Engineering 98: Proceedings of the International Water Resources Engineering Conference*. Sponsored by The Water Resources Engineering Division of the American Society of Civil Engineers, co-sponsored by the U.S. Geological Survey, vol. 2, 1739–1744.

Yuan, H. 1997. Investigation of single-phase liquid flow behavior in horizontal wells. Ph.D. diss., University of Tulsa, Tulsa, Oklahoma.

Yuan, H., Sarcia, C., and Brill, J. 1999. Effect of perforation density on single-phase liquid flow behavior in horizontal wells. *SPE Production & Facilities* 14, no. 3: 203–209.

Appendix A

Implementation within MODFLOW

In this appendix, the equations of flow as implemented in the MODFLOW model are described. The model is axially symmetric. Columns are used to define radial positions and layers are used for elevation. Figure A1 presents a small example of an axially symmetric aquifer-borehole model. Column 1 represents the borehole, which is depicted in blue in the figure. The width of column 1 would be the inner radius of the well screen. The aquifer formation is shown in brown. The aquifer extends from column 3 to the outer edge of the model domain. There are two regions shown in column 2. The red region of layers 3 and 4 depicts a borehole screen with the column width set to the width of the screen. The cross-hatched region of layers 1 and 2 represents a solid well casing. The model cells of column 2 of layers 1 and 2 would be inactive.

Flow in Wellbore

For the MODFLOW model, the flow between layers in the wellbore is

$$Q = CV\Delta h_{\mathrm{v}} \tag{A1}$$

where Q is the flow rate between layers, CV is the vertical conductance between layers (Harbaugh et al. 2000), and Δh_{v} is the head difference between the layers of the model. We can determine the velocity at a layer interface $\acute{V}$ as

$$\acute{V} = \frac{Q}{A_{\mathrm{w}}} \tag{A2}$$

where $A_{\mathrm{w}} = \pi r_{\mathrm{w}}^2$. Equation A2 provides the determination of CV from the head difference of Equation 18 as

$$CV = \frac{A_{\mathrm{w}}\acute{v_b}}{\Delta h} \tag{A3}$$

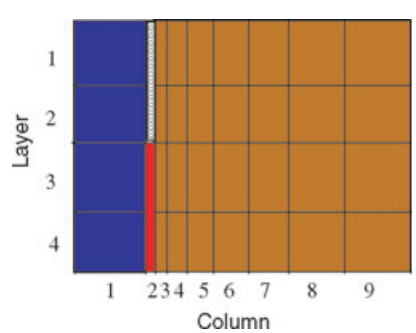

Figure A1. Schematic diagram of a small aquifer-borehole model. The blue region is open borehole, red is borehole screen, and brown is aquifer material. The cross-hatching represents inactive model cells of a solid casing.

Δh is the head drop calculated from the conservation of momentum equations. For both Equations A1 and A3 to be true, $\Delta h_v = \Delta h$. By iteratively using Equation A3 to redefine CV and then re-solving for Δh_v using MODFLOW, Equation A3 converges to a head solution consistent with Equation 18 even from poor, but not all, starting estimates of the initial CV value. Failure to converge is rare enough than it is a nuisance rather than a serious problem.

Substituting Equation 18 for Δh results in

$$CV = \frac{A_w \acute{V}}{\frac{\beta_2 V_2{}^2}{g} - \frac{\beta_1 V_1^2}{g} - \frac{1}{4gr_w}\int_{z_1}^{z_2} f\, V^2 \mathrm{d}z} \tag{A4}$$

where V_1 is defined at the lower node location and V_2 is defined at the upper node location. These velocities are related to the velocity at the boundary through the average inflow through screens.

$$\begin{aligned} V_1 &= \acute{V} - \frac{\Delta z_1}{r_w} v_{r1} \\ V_2 &= \acute{V} + \frac{\Delta z_2}{r_w} v_{r2} \end{aligned} \tag{A5}$$

where Δz_i is the thickness of layer i. The average inflow velocity is defined by

$$v_{ri} = \frac{CR\Delta h_r}{2\pi r_w \Delta z_i} \tag{A6}$$

where CR is the radial conductance between the well and the first column of the formation within the cylindrical geometry MODFLOW model (Clemo 2002). This velocity is treated as constant within a layer. We now have the definitions to evaluate the last term of Equation 18 for any of three flow regimes: laminar, transition, and turbulent. The development is presented as if the flow regime is the same for both layers between nodes, but within the code each layer is evaluated independently based on the largest Reynolds number in the layer.

Using Equation 14, the shear term between node locations becomes for laminar flow

$$\begin{aligned} &\frac{1}{4gr_w}\int_{z_1}^{z_2} f\, V^2 \mathrm{d}z \\ &= \frac{f_0}{4gr_w}\int_{z_1}^{z_2} V^2 \mathrm{d}z + \frac{1}{4gr_w}\int_{z_1}^{z_2} \frac{64\nu}{gr_w^2} V \mathrm{d}z \end{aligned} \tag{A7}$$

The first term, for laminar flow in the two layers, evaluates to

$$\begin{aligned} &\frac{f_0}{4gr_w}\int_{z_1}^{z_2} V^2 \mathrm{d}z \\ &= \frac{f_0}{4gr_w}\left[\int_{z_1}^{\acute{z}} \left(\acute{V} - \frac{v_{r1}\Delta z_1}{r_w} + \frac{2v_{r1}}{r_w} z\right)^2 \mathrm{d}z \right. \\ &\quad \left. + \int_{\acute{z}}^{z_2} \left(\acute{V} + \frac{2v_{r2}}{r_w} z\right)^2 \mathrm{d}z \right] \\ &= \frac{f_0}{4gr_w}\left[\Delta z_1 \acute{V}^2 - \frac{\acute{V} v_{r1} (\Delta z_1)^2}{2r_w} \right. \\ &\quad \left. + \frac{1}{3}\frac{v_{r1}^2 (\Delta z_1)^3}{r_w^2}\right] \\ &\quad + \frac{f_0}{4gr_w}\left[\Delta z_2 \acute{V}^2 + \frac{\acute{V} v_{r2} (\Delta z_2)^2}{2r_w} \right. \\ &\quad \left. + \frac{1}{3}\frac{v_{r2}^2 (\Delta z_2)^3}{r_w^2}\right] \end{aligned} \tag{A8}$$

The second term becomes

$$\begin{aligned} &\frac{1}{4gr_w}\int_{z_1}^{z_2} \frac{64\nu}{gr_w^2} V \mathrm{d}z \\ &= \frac{4\nu}{gr_w^2}\left[\int_{z_1}^{\acute{z}} \left(\acute{V} - \frac{v_{r1}\Delta z_1}{r_w} + \frac{2v_{r1}}{r_w} z\right) \mathrm{d}z \right. \\ &\quad \left. + \int_{\acute{z}}^{z_2} \left(\acute{V} + \frac{2v_{r2}}{r_w} z\right)\right] \mathrm{d}z \\ &= \frac{4\nu\Delta z_1}{gr_w^2}\left[\acute{V} - \frac{\Delta z_1}{2r_w} v_{r1}\right] \\ &\quad + \frac{4\nu\Delta z_2}{gr_w^2}\left[\acute{V} + \frac{\Delta z_2}{2r_w} v_{r2}\right] \end{aligned} \tag{A9}$$

In the transition region between laminar and turbulent flow regimes, we have

$$\begin{aligned} &\frac{1}{4gr_w}\int_{z_1}^{z_2} f V^2 \mathrm{d}z \\ &= \frac{f_0 + 0.028}{4gr_w}\int_{z_1}^{z_2} V^2 \mathrm{d}z + \frac{f_t(\epsilon, 3400) - 0.028}{0.708 gr_w} \\ &\quad \times \int_{\acute{z}}^{z_2} \log\left(\frac{d_h\left(\acute{V} - \frac{v_{r1}\Delta z_1}{r_w} + \frac{2v_{r1}}{r_w} z\right)}{\nu}\right) \\ &\quad \times \left(\acute{V} - \frac{v_{r1}\Delta z_1}{r_w} + \frac{2v_{r1}}{r_w} z\right)^2 \mathrm{d}z \\ &\quad + \frac{f_t(\epsilon, 3400) - 0.028}{0.708 gr_w} \\ &\quad \times \int_{z_1}^{\acute{z}} \log\left(\frac{d_h\left(\acute{v_b} + \frac{2v_{r2}}{r_w} z\right)}{\nu}\right) \\ &\quad \times \left(\acute{v_b} + \frac{2v_{r2}}{r_w} z\right)^2 \mathrm{d}z \end{aligned} \tag{A10}$$

The first term in Equation A10, is similar to the first term of laminar flow. The second two terms can be transformed to a form

$$\begin{aligned} &\frac{f_t(\epsilon, 3400) - 0.028)}{0.708 gr_w}\frac{r_w}{2v_r} \\ &\quad \times \int_{v_{b1}}^{v_{b2}} \left[\left(\log\left(\frac{d_h}{\nu}\right) + \log(V)\right) V^2\right] \mathrm{d}V \end{aligned} \tag{A11}$$

that reduces to

$$\frac{f_t(\epsilon, 3400) - 0.028)}{0.708 g r_{\mathrm{w}}} \frac{r_{\mathrm{w}}}{6 V_{\mathrm{s}}} \left[V_2^3 \left(\log(Re_2) - \frac{1}{3} \right) - V_1^3 \left(\log(Re_1) - \frac{1}{3} \right) \right] \quad \text{(A12)}$$

To evaluate f, Siwoń (1987) used the Altshul approximation (Altshul and Kiselev 1975; ASHRAE 1997) for the Colebrook-White formula in the turbulent smooth region.

$$f = 0.11 \left(\epsilon + \frac{68}{Re} \right)^{0.25} \quad \text{(A13)}$$

This formula is reported to be accurate to within 1.6% (ASHRAE 1997). We use the more accurate Chen formula (Chen 1979; Ouyang and Aziz 1996):

$$\sqrt{\frac{1}{f}} = -2\log \left[\frac{\epsilon}{3.7065} - \frac{5.0452}{Re} \times \log \left(\frac{\epsilon^{1.1098}}{2.8257} + \frac{7}{Re^{0.8981}} \right) \right] \quad \text{(A14)}$$

Wellbore Screen

Equation 18 can be generalized for an arbitrary length of well screen that is large compared to the slot spacing by approximating the average inflow velocity across the screen as

$$\begin{aligned} v_r &= \frac{\theta \alpha_r (z_{s1} - z_{s2})}{\Delta z_{\mathrm{s}}} V_{\mathrm{s}} \quad \text{(A15)} \\ &= \theta \phi V_{\mathrm{s}} \end{aligned}$$

where Δz_{s} is the spacing of the slots. The screen porosity, the fraction of screen open to flow, and the hydraulic radius used to calculate the friction factor, f_{s} (Equation 22), are input parameters to the model. These factors provide the ability to represent a skin effect due to partial clogging of the wellbore screen that we believe exists at one of our study sites (Barrash et al. 2006).

Nomenclature

- A Cross-sectional area of the outside of the slot
- A_1 Narrowest cross section of an orifice
- A_2 Effective cross section of area of flow that contracts into the slot
- A_s Nomenclature of cross section of slot used by Cooley and Cunningham (1979)
- A_{w} Cross-sectional area of wellbore
- α_r Fraction of the screen radius where there are slots open to flow, ignoring potential clogging
- β Momentum factor
- Cir Circumference of the well screen at its radial midpoint
- C_{d} Discharge coefficient for an orifice
- C_{v} Velocity coefficient for flow through an orifice
- C_E Klotz's friction factor correction factor for slots
- CR Radial conductance between cells of MODFLOW
- CV Vertical conductance between cells of MODFLOW
- d_h Hydraulic diameter
- ϵ_p Pipe roughness—ratio of wall surface roughness to pipe radius
- ϵ Effective pipe roughness of well screen
- η Siwoń's momentum function for inflow
- f Friction factor
- f_0 Constant friction factor term to account for existence of slot openings
- f_t Velocity dependent friction factor term to account for existence of slot openings
- g Gravitational acceleration
- h Hydraulic head
- Δh_{v} Hydraulic head difference between two cells of MODFLOW
- γ Angle of radial flow in the well bore at r_{w}
- $\overline{\gamma}$ Effective average γ of flow entering wellbore from slot
- ν Kinematic viscosity of the fluid
- p Fluid pressure
- Q Volumetric flow rate between two cells of MODFLOW
- r Radial distance from the center of the wellbore
- Re Reynolds number
- ρ Fluid density
- ϕ Screen porosity—fraction of screen that is slot
- ψ Form factor for slot
- τ Shear stress of fluid at r_{w}
- θ Fraction of slot that is open to flow
- v Fluid velocity at a point
- V Average (bulk) fluid velocity
- $\acute{V}$ Vertical fluid velocity at the boundary between two cells
- W_s Width of slot—perpendicular to radial direction
- z Elevation—axial coordinate

Subscripts

- 1 Bottom; alternately the lower layer
- 2 Top; alternately the upper layer
- cl Center of the wellbore
- r Radial direction
- s Slot
- z Vertical direction
- w Just inside the screen